SUPPLEMENTARY INFORMATION

Endogenous retrovirus-derived lncRNA *BANCR* promotes cardiomyocyte migration in humans and non-human primates

Kitchener D. Wilson,[1,2]† Mohamed Ameen,[1,3]† Hongchao Guo,[1]† Oscar J. Abilez,[1] Lei Tian,[1] Maxwell R. Mumbach,[4] Sebastian Diecke,[5] Xulei Qin,[1] Yonggang Liu,[1] Huaxiao Yang,[1] Ning Ma,[1] Sadhana Gaddam,[4] Nathan Cunningham,[1] Mingxia Gu,[1] Evgenios Neofytou,[1] Maricela Prado,[1] Thomas B. Hildebrandt,[6] Ioannis Karakikes,[1,7] Howard Y. Chang,[4] Joseph C. Wu[1,8]

[1]Cardiovascular Institute, Stanford University, Stanford, CA 94305, USA.

[2]Department of Pathology, Stanford University, Stanford, CA 94305, USA.

[3]Department of Cancer Biology, Stanford University, Stanford, CA 94305, USA.

[4]Center for Personal Dynamic Regulomes and Program in Epithelial Biology, Stanford

[5]Berlin Institute of Health, Max Delbrück Center, and DZHK (German Center for Cardiovascular Research), Berlin, Germany.

[6]Wildlife Reproduction Medicine, Freie University, and Leibniz Institute for Zoo and Wildlife Research, Berlin, Germany.

[7]Department of Cardiothoracic Surgery, Stanford University, Stanford, CA 94305, USA.

[8]Departments of Medicine and Radiology, Stanford University, Stanford, CA 94305, USA.

† These authors contributed equally to this work.

Correspondence: joewu@stanford.edu (J.C.W.), kitch.wilson@gmail.com (K.D.W.)

Lead Contact: joewu@stanford.edu (J.C.W.)

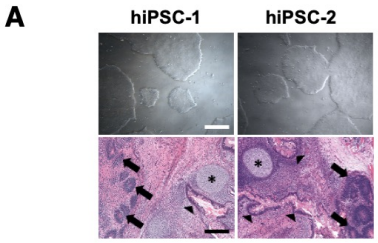

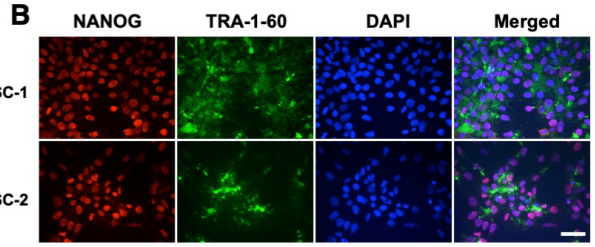

C

Fetus-1 WES

gene	dbSNP	ref_base	alt_base	hom_het	region	change	ExAC total allele freq	ClinVar
TTN	rs77419653	C	T	het	exonic	nonsynonymous_SNV	0.006226	Benign/Likely benign
TTN	rs3813246	T	C	het	exonic	nonsynonymous_SNV	0.02616	Benign/Likely benign
TTN	rs56018860	T	C	het	exonic	nonsynonymous_SNV	0.02618	Benign/Likely benign
TTN	rs72648257	T	C	het	exonic	nonsynonymous_SNV	0.02619	Benign/Likely benign
TTN	rs3813245	A	G	het	exonic	nonsynonymous_SNV	0.02621	Benign/Likely benign
TTN	rs3731745	A	G	het	exonic	nonsynonymous_SNV	0.02626	Benign/Likely benign
TTN	rs55675869	C	T	het	exonic	nonsynonymous_SNV	0.02882	Benign/Likely benign
TTN	rs2288563	T	C	het	exonic	nonsynonymous_SNV	0.02912	Benign/Likely benign
TTN	rs2303832	T	A	het	exonic	nonsynonymous_SNV	0.02916	Benign/Likely benign

Fetus-2 WES

gene	dbSNP	ref_base	alt_base	hom_het	region	change	ExAC total allele freq	ClinVar
AKAP9	rs142401936	C	T	het	exonic	nonsynonymous_SNV	0.001662	Benign/Likely benign
TRDN	rs192289289	C	T	het	exonic	nonsynonymous_SNV	0.007306	Benign
SYNE1	rs111449472	A	G	het	exonic	nonsynonymous_SNV	0.0113	Benign/Likely benign
FKTN	rs34006675	G	A	het	exonic	nonsynonymous_SNV	0.01532	Benign
MYPN	rs62620248	G	A	het	exonic	nonsynonymous_SNV	0.01838	Benign
BAG3	rs35434411	G	A	het	exonic	nonsynonymous_SNV	0.02012	Benign/Likely benign
DMD	rs1800273	G	A	het	exonic	nonsynonymous_SNV	0.02605	Benign/Likely benign

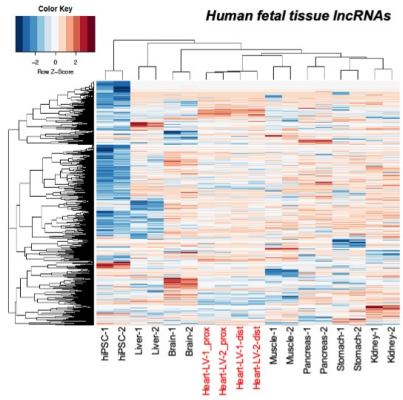

E

	LincRNAs and TUCPs with specific expression in fetal heart	Annotation	hg19 genome coordinates
1	TCONS_00006505	lincRNA	chr3:46876675-46888307:-
2	TCONS_00014514	lincRNA	chr8:54427731-54436491:-
3	TCONS_00020726+TCONS_00021293+TCONS_00020727	lincRNA	chr12:20257338-20262820:-
4	**BANCR**	**lincRNA**	**chr9:71911597-71921972:-**
5	TCONS_00020859	lincRNA	chr12:83850418-83866379:-
6	TCONS_00010558	lincRNA	chr5:172663704-172671727:-
7	TCONS_00008091+TCONS_00008798+TCONS_00008799+TCONS_00008800+TCONS_00008801	lincRNA	chr4:62999462-63027983:+
8	TCONS_l2_00003843+TCONS_l2_00004301+TCONS_l2_00003844	TUCP	chr10:134309449-134350303:-
9	TCONS_00028451	lincRNA	chr20:55733858-55737430:-
10	TCONS_00024710+TCONS_00025039	lincRNA	chr16:66931240-66934554:-
11	TCONS_00004738+TCONS_00004739+TCONS_00002863+TCONS_00002691+TCONS_00004740+TCONS_00003621+TCONS_00003622	lincRNA	chr2:30555416-30583316:+
12	TCONS_00007450+TCONS_00009188+TCONS_00008689+TCONS_00009189+TCONS_00009190+TCONS_00008690+TCONS_00008691+TCONS_00008692	lincRNA	chr4:185286341-185303530:-
13	TCONS_00008880	lincRNA	chr4:123621606-123629294:+
14	TCONS_l2_00028124+TCONS_l2_00028126	TUCP	chr8:23569205-23584509:-
15	TCONS_00014103+TCONS_00014104+TCONS_00012991+TCONS_00012875+TCONS_00012992+TCONS_00012876+TCONS_00013411	lincRNA	chr7:35755720-35774497:+
16	TCONS_00010554+TCONS_00011086+TCONS_00011087	lincRNA	chr5:171150035-171164435:-
17	TCONS_l2_00007025	TUCP	chr13:114053727-114064046:+

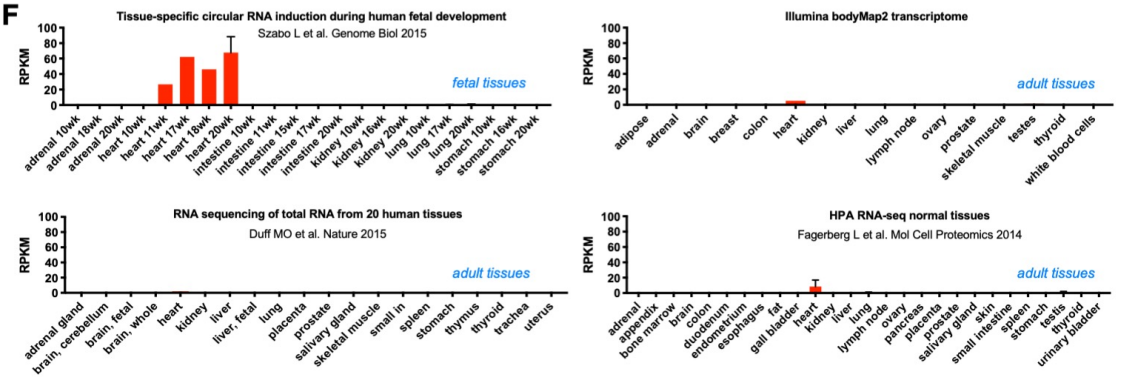

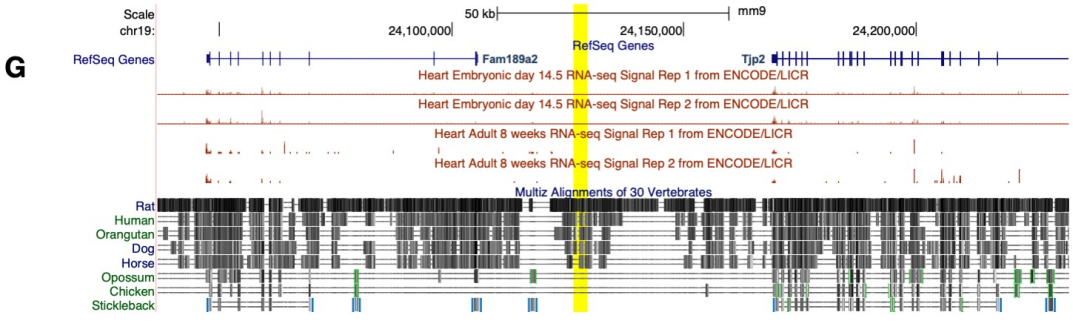

Supplementary Figure 1

Supplementary Fig. 1. Fetal heart specific expression of *BANCR*. Related to Fig. 1. (**A**) Top panels - Brightfield images of hiPSC-1 and hiPSC-2 (derived from Fetus-1 and Fetus-2, respectively) show typical embryonic colony morphology. Scale bar = 200 μm. Bottom panels - H&E staining of teratomas derived from hiPSC-1 and hiPSC-2. Immature neural tissue (arrows); intestinal type epithelium (arrowheads); and cartilage (asterisk). Scale bar = 300 μm. (**B**) Immunostaining for pluripotency markers (NANOG, TRA-1-60) of hiPSC-1 and hiPSC-2. Scale bar = 30 μm. (**C**) Whole exome sequencing (WES) from Fetus-1 and Fetus-2 reveals no known non-synonymous exonic mutations in genes related to cardiomyopathy, channelopathy, or congenital heart diseases were detected. (**D**) Heatmap showing Pearson correlation hierarchical clustering of fetal tissues and hiPSCs. One-way ANOVA, *P* value < 0.05. (**E**) Table of fetal heart-specific lincRNA and TUCP expression (see Fig. 1B for correlated heatmap). A unique transcript for each lincRNA or TUCP was created by merging overlapping exons into one unique exon, which resulted in merged identifiers. (**F**) Independent RNA-seq studies of human adult and fetal tissues confirm heart-specific expression of *BANCR*, with predominant expression in fetal hearts compared to adult hearts. Error bars are +/- 1 s.d. (**G**) UCSC genome browser screenshot of ENCODE RNA-seq data for fetal and adult mouse hearts shows no transcription in Liftover-predicted orthologous *BANCR* region (mm9 chr19:24126270-24129257, yellow highlight). $n = 2$ biological replicates of 8 week murine adult hearts, $n = 2$ biological replicates of E14.5 murine embryo heart.

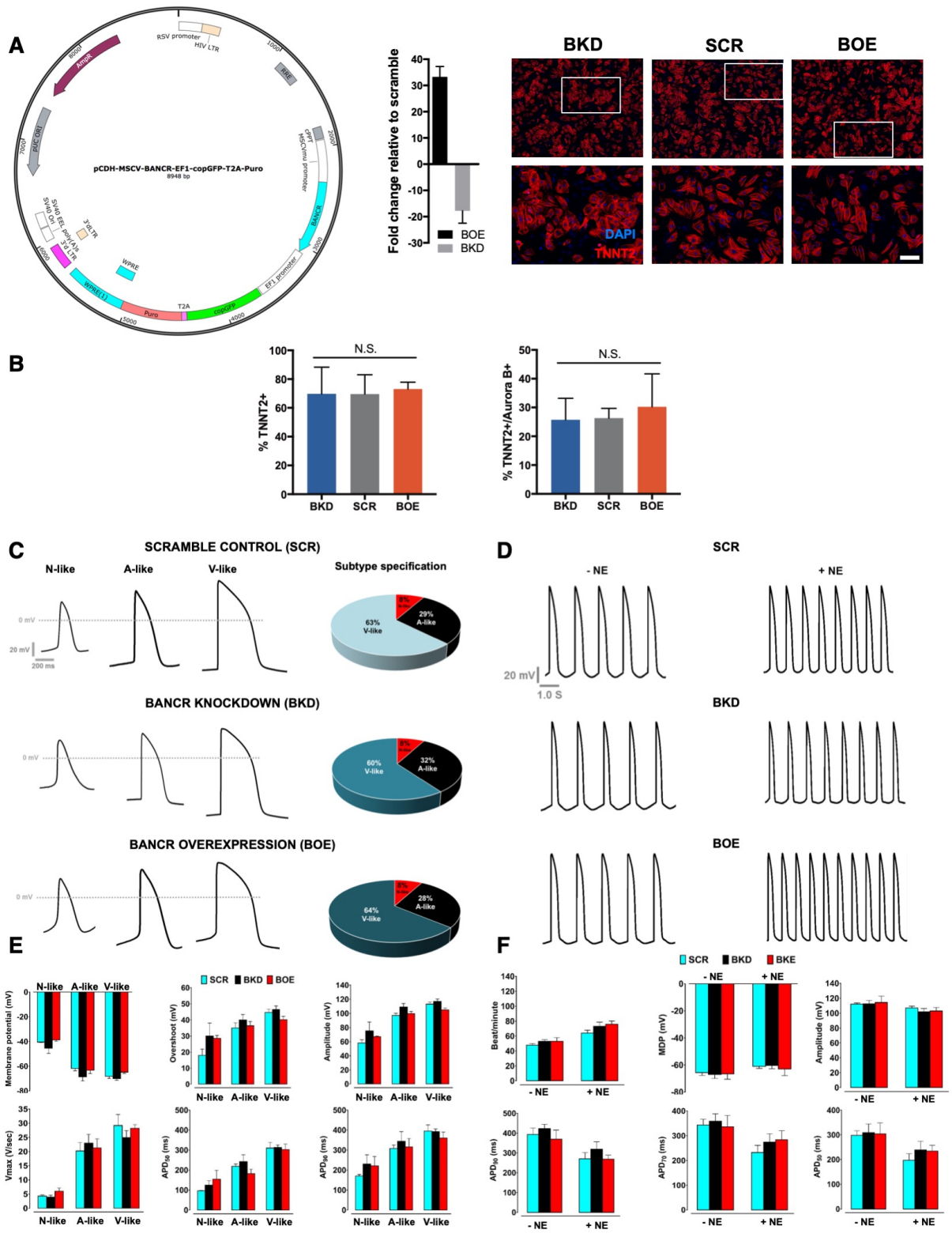

Supplementary Figure 2

Supplementary Fig. 2. *BANCR* knockdown and over-expression does not affect sarcomeric or electrophysiological properties of hESC-CMs. Related to Fig. 3. (**A**) Plasmid map of the over-expression vector (left panel), qPCR confirmation of *BANCR* over-expression and knockdown (middle panel, n = 5 biological replicates), and TNNT2/DAPI immunostaining of *BANCR* knockdown (BKD), scramble control (SCR), and *BANCR* over-expression (BOE) hESC-CMs (right panel). Error bars are +/- 1 s.d. Scale bar = 50 μm. (**B**) FACS of TNNT2 and Aurora B immunostaining in hESC-CMs. P value < 0.05, one-way ANOVA; N.S., not significant. n = 3 biological replicates, error bars are +/- 1 s.d. (**C**) Representative action potential (AP) recordings and subtype distribution using whole cell patch clamping of three major CM subtypes: SCR (n = 24), BKD (n = 25), and BOE (n = 25). Cells exhibit AP morphologies that can be categorized as nodal (N)-, atrial (A)-, or ventricular (V)-like CMs. (**D**) Patch clamp recordings of hESC-CMs demonstrating maximal diastolic potential (MDP), action potential amplitude (APA), overshoot/peak voltage, V_{max} (maximal rate of depolarization), APD_{50}, and APD_{90}. (**E**) Representative action potential (AP) recordings showing the effect of 1 μM norepinephrine (NE) on SCR (n = 5), BKD (n = 5), and BOE (n = 5) hESC-CMs using whole-cell patch clamp. (**F**) Patch clamp recordings of hESC-CMs demonstrating beating rate, MDP, APA, overshoot/peak voltage, APD_{50}, APD_{70}, and APD_{90}. No significant differences among the three groups for any of above electrophysiologic parameters were observed. P value < 0.05, one-way ANOVA. Error bars are +/- 1 s.d.

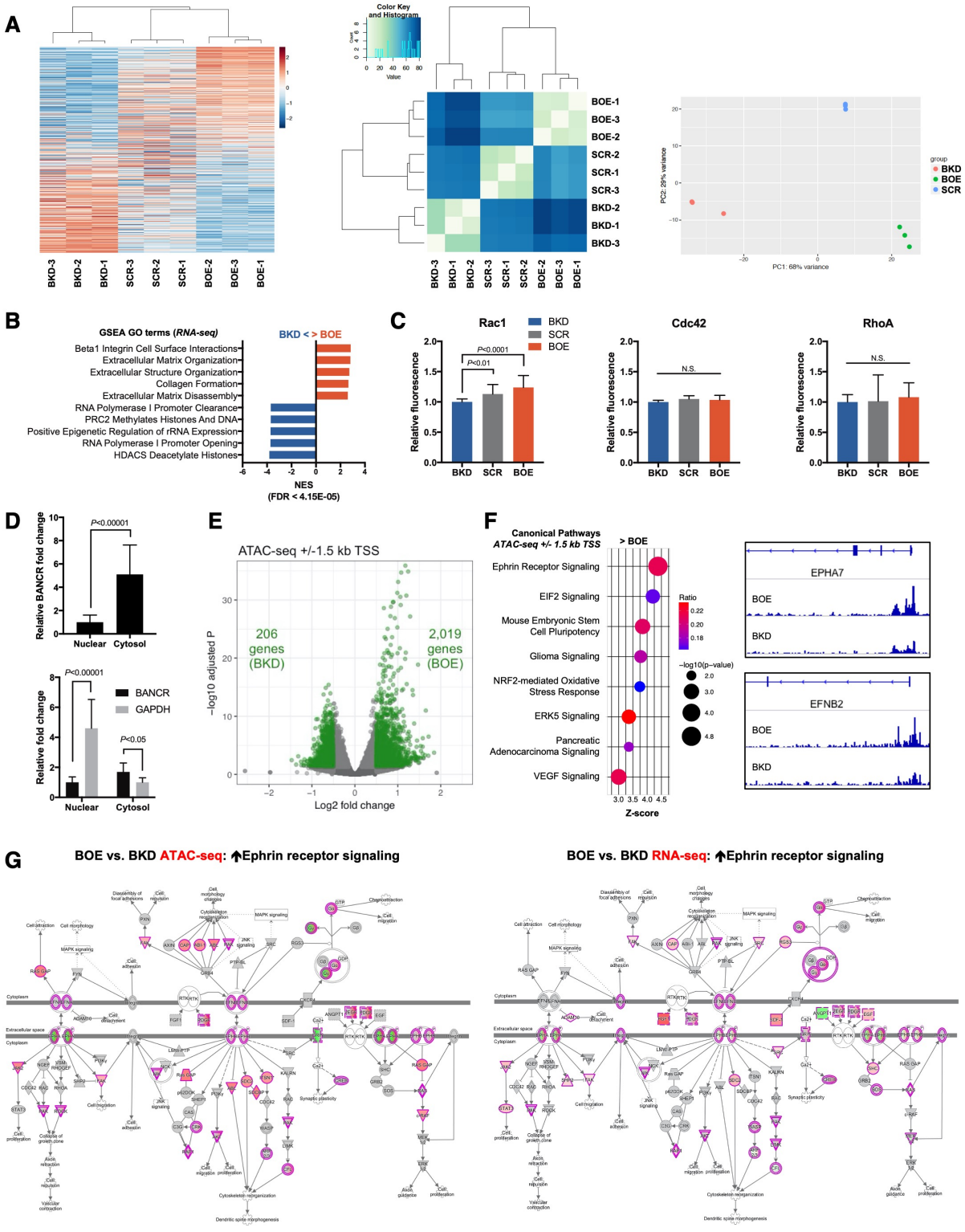

Supplementary Figure 3

Supplementary Fig. 3. RNA- and ATAC-seq of *BANCR* knockdown and over-expression in hESC-CMs. Related to Fig. 3. (**A**) RNA-seq heatmap showing all expressed genes across BOE (*BANCR* over-expression), BKD (*BANCR* knockdown), and SCR (scramble control) hESC-CMs (left panel). Pairwise correlation heatmap (middle panel). Principal component analysis (PCA) of RNA-seq data showing distinct variation among BOE, BKD, and SCR hESC-CM groupings (right panel). (**B**) GSEA of RNA-seq data reveals significant enrichment of β1 integrin, extracellular matrix organization, and collagen formation in BOE hESC-CMs. In contrast, BKD hESC-CMs are enriched for histone deacetylase (HDAC) and RNA polymerase pathways. Gene Ontology (GO) terms (FDR = 0) with the top 5 normalized enrichment scores (NES) in both BKD and BOE are shown. (**C**) ELISA quantification of GTP-bound Rho GTPase proteins in hESC-CMs shows activation of Rac1 but not Cdc42 or RhoA. P value < 0.05, two sided t-test. n = 4 biological replicates, error bars are +/- 1 s.d. BKD hESC-CMs exhibit the lowest GTP-bound Rho GTPase protein, indicating lowest Rac1 activation, relative to SCR and BKD hESC-CMs. (**D**) *BANCR* is found in both nuclear and cytoplasmic fractions by qPCR analysis, with predominance in cytosol (top). GAPDH shown for comparison (bottom). Two-tailed t-test. n = 5 biological replicates, error bars are +/- 1 s.d. (**E**) Volcano plot of ATAC-seq data at TSS +/- 1.5 kb. $|\text{Log}_2(\text{fold change})| > 0.5$, Benjamini-Hochberg-adjusted P value < 0.05. n = 2 biological replicates. (**F**) Increased open chromatin at promoters of ephrin receptor signaling genes in BOE hESC-CMs. Ephrin receptor signaling is known to regulate cellular migration. Note that ephrin receptor signaling was also seen in our RNA-seq results (see below). Benjamini-Hochberg-adjusted $-\log_{10}P$ value > 2, Z score > 3. Right panels show example IGV screenshots of promoter regions for EPHA7 (ephrin receptor) and EFNB2 (ephrin ligand) that are key factors in ephrin receptor signaling. (**G**) IPA network diagrams show increased promoter chromatin accessibility (ATAC-seq TSS +/- 1.5 kb) and gene expression (RNA-seq) in ephrin receptor signaling pathway. Taken together, both modalities (ATAC- and RNA-seq) suggest Ephrin receptor signaling may be one important pathway related to *BANCR* expression. Colored molecules in diagrams indicate significantly changed chromatin accessibility or gene expression. $|\text{Log}_2(\text{fold change})| > 0.5$, Benjamini-Hochberg-adjusted P value < 0.05.

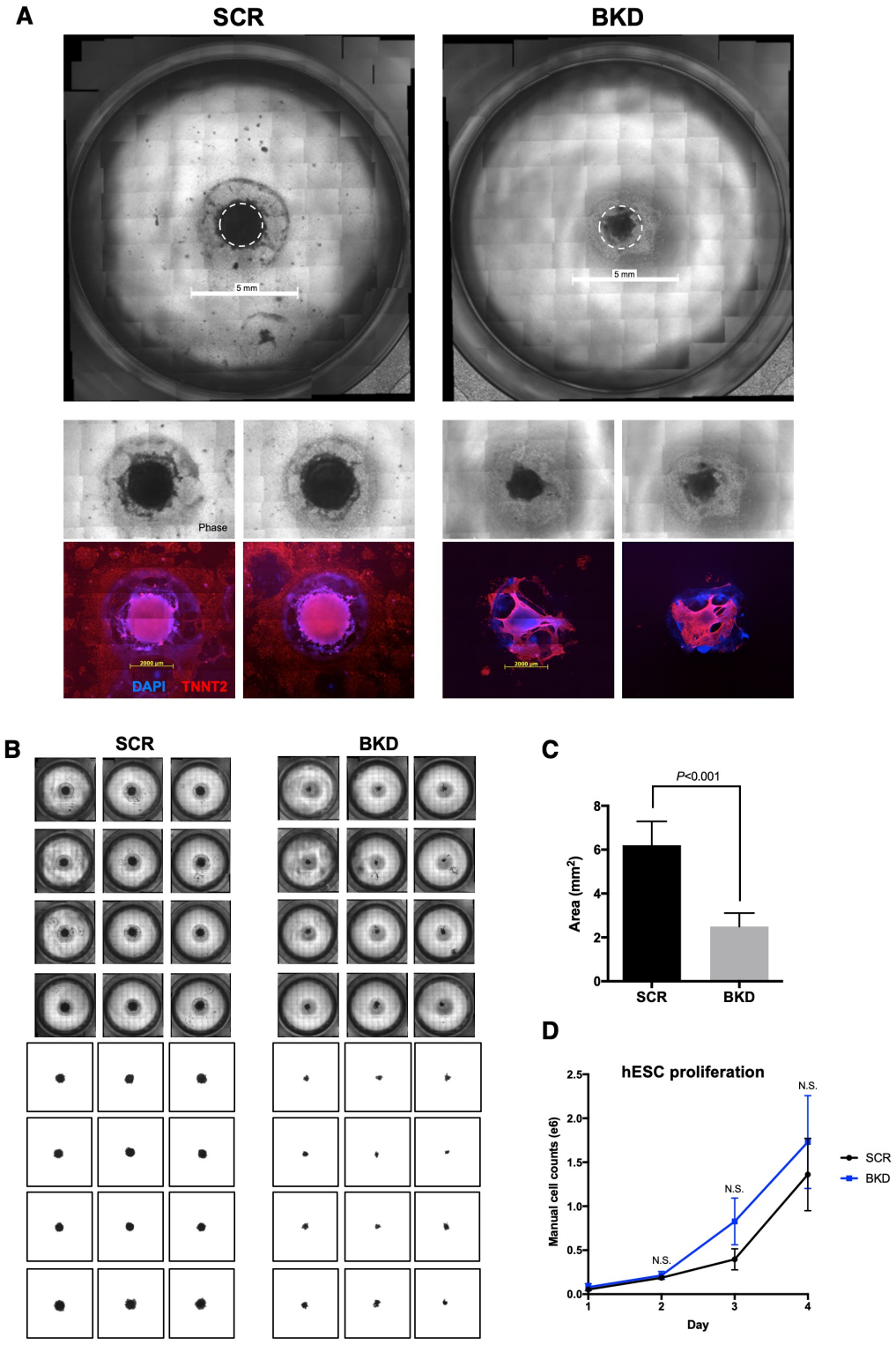

Supplementary Figure 4

Supplementary Fig. 4. BKD cardioids exhibit smaller and more disorganized morphologies compared to SCR control. Related to Fig. 3F. (**A**) Representative images of beating micropatterns after 14 days of cardiac differentiation in 24-well plates. Dashed circles in top panels indicate original starting size of hESC micropattern (2 mm diameter). BKD cardioids are significantly contracted compared to scramble (SCR) control cardioids, reflecting their lost migratory potential. (**B**) Image removal of background emphasizes smaller size of BKD micropatterns. (**C**) Quantification of SCR vs. BKD micropattern sizes. Quantitatively, BKD cardioids are significantly smaller than SCR cardioids reflecting their reduced migration. Two-tailed *t*-test. $n = 36$ biological replicates, error bars are +/- 1 s.d. (**D**) To rule out possibility of increased proliferation in undifferentiated BKD and SCR hESCs, daily manual cell counts were performed for 4 days. P value < 0.05, two-tailed *t*-test. $n = 3$ biological replicates at each time point. Error bars are +/- 1 s.d.

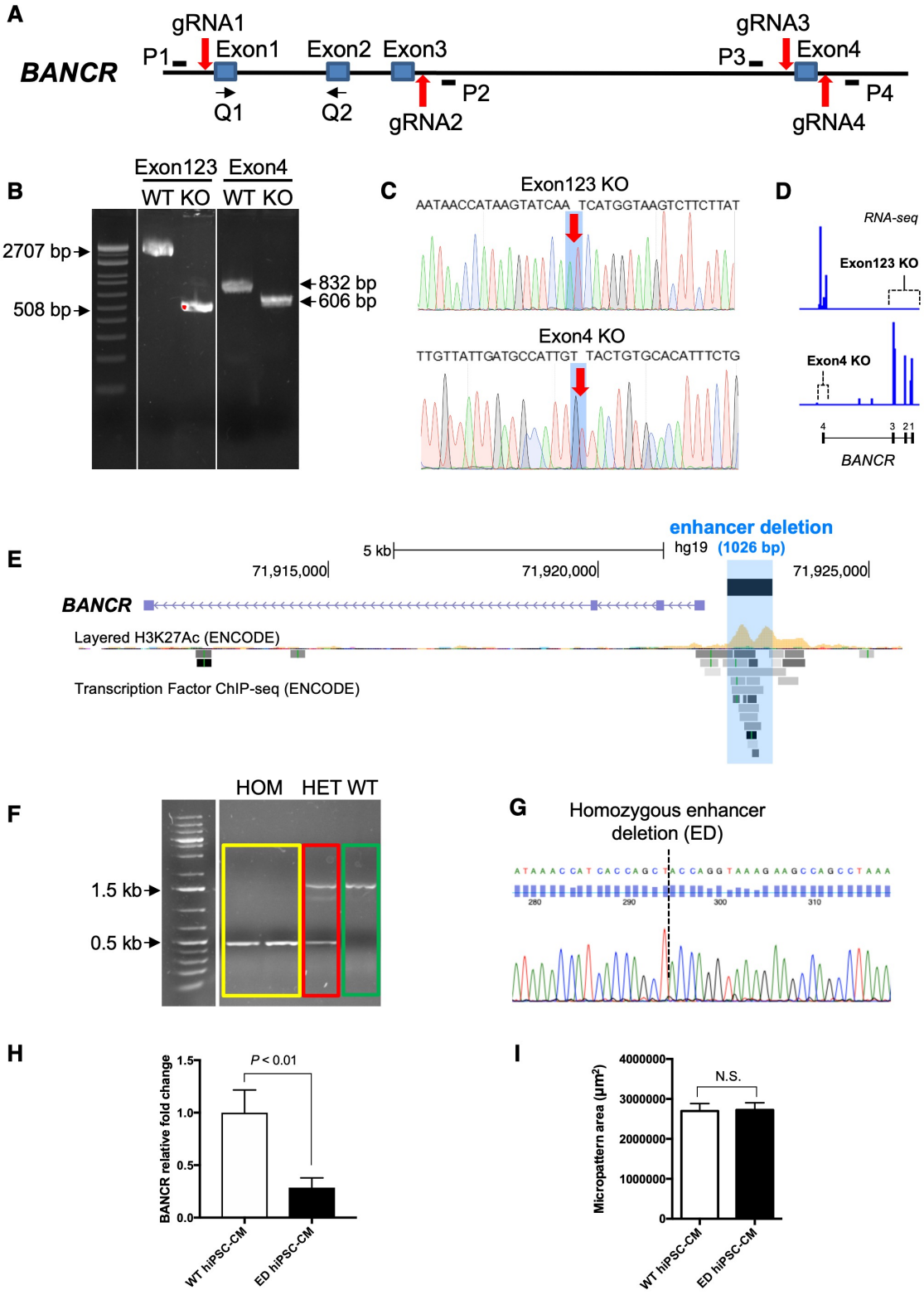

Supplementary Figure 5

Supplementary Fig. 5. CRISPR/Cas9 targeted deletion of *BANCR* exons and enhancer. Related to Figs. 4 and 5. (**A**) Schematic of *BANCR* exons 1-4 depicting the two CRISPR/Cas9-targeted regions (exons 1-3 and exon 4) and associated PCR primers (note that Q1 and Q2 indicate qPCR primers used for quantifying *BANCR* expression). (**B**) PCR confirmation of homozygous knockout (KO) in Exon123 (primers P1 and P2) and Exon4 (primers P3 and P4) but not wildtype (WT) hESCs. (**C**) Sanger sequencing confirms homozygous deletions in both cell lines at the appropriate loci (red arrows), respectively. (**D**) IGV screenshots of RNA-seq expression data at *BANCR* locus in hESC-CMs confirms loss of the appropriate exon(s). (**E**) UCSC screenshot of *BANCR* with accompanying ENCODE tracks showing layered H3K27ac ChIP-seq and transcription factor binding loci identified through ChIP-seq studies. Highlighted region shows the 1,026 bp locus overlying the upstream enhancer that was deleted with CRISPR/Cas9. (**F**) PCR confirmation of homozygous (HOM) and heterozygous (HET) deletion of ~1 kb fragment but not wildtype (WT) hiPSCs. (**G**) Sanger sequencing confirms homozygous deletion (dashed line). (**H**) qPCR shows downregulation of *BANCR* expression in ED hiPSC-CMs relative to isotype WT control cells. Two sided *t*-test. $n = 3$ biological replicates, error bars are +/- 1 s.d. (**I**) Beating micropatterns after two weeks of culture show no change in size (quantified by TNNT immunostaining) between WT and ED hiPSC-CMs. $n = 2$ biological replicates (32 micropatterns per group), error bars are +/- 1 s.d.

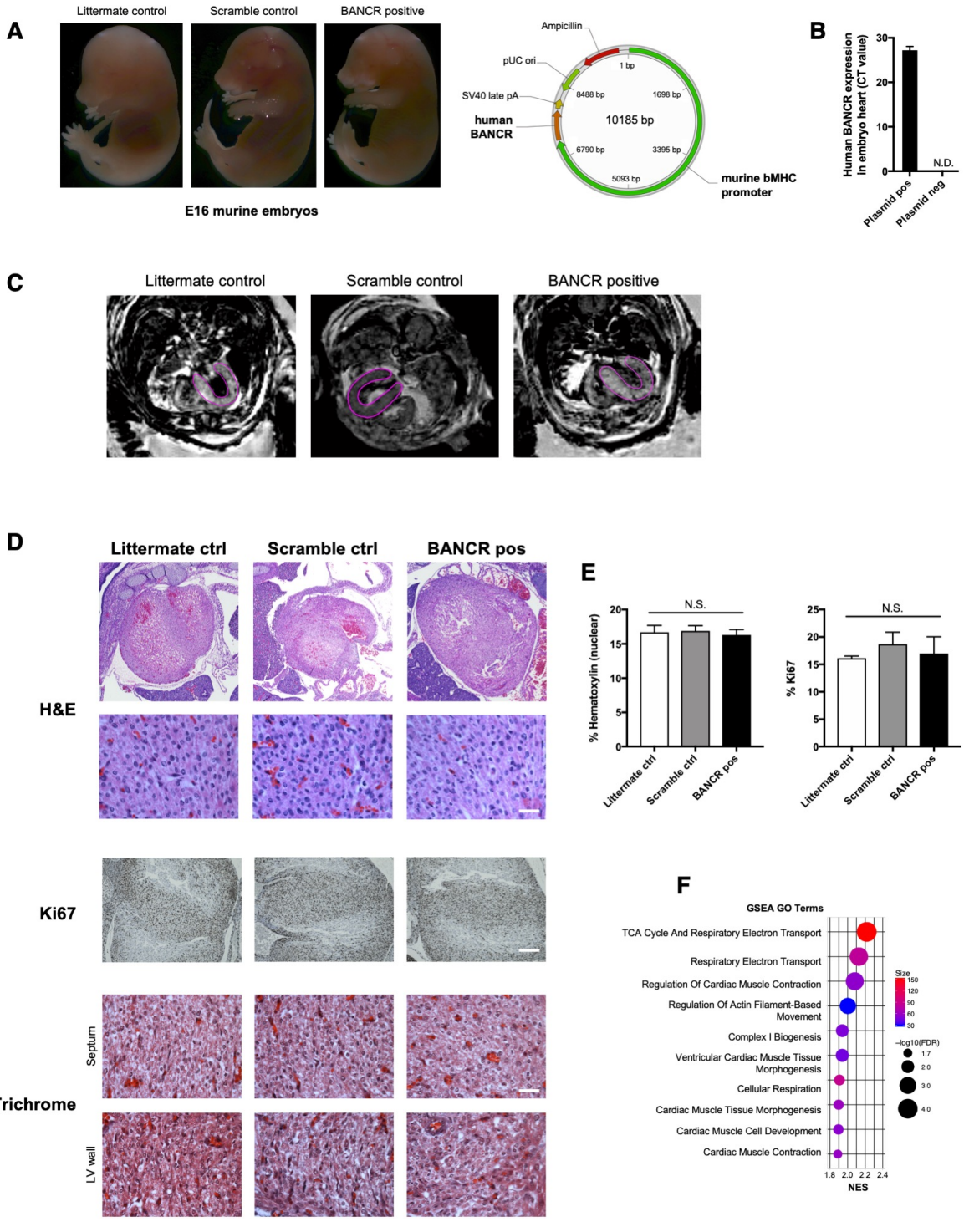

Supplementary Figure 6

Supplementary Fig. 6. *BANCR* knock-in murine embryos. Related to Fig. 7H. (**A**) Left panel: representative *BANCR* positive E16 FVB murine embryos (*n* = 9 biological replicates), scramble (*n* = 6 biological replicates), and PCR-negative (*n* = 13 biological replicates) littermate controls, generated using plasmid pronuclear injection prior to implantation and subsequent harvest. Right panel: The plasmid map showing beta Myosin Heavy Chain promoter (*bMHC*, also known as *MYH7*) that is primarily active in fetal mouse heart and drives fetal heart expression of human *BANCR* (or scramble) cDNA. (**B**) Plasmid-positive embryos express human *BANCR* in heart tissue. N.D., not detected. *n* = 3 biological replicates, error bars are +/- 1 s.d. (**C**) Representative magnetic resonance imaging (MRI) of cross-sections with demarcated left ventricles shown. (**D**) H&E (scale bar = 40 μm), Ki67 (scale bar = 200 μm), and Trichrome (scale bar = 40 μm) staining of embryo hearts. No differences in Ki67 are seen, indicating that *BANCR*+ cardiomyocytes are not overtly proliferating at this embryonic stage (ventricular septa of representative hearts are shown for comparison). Trichrome staining demonstrates no differences in fibrosis or scar formation. Representative images of left ventricular (LV) wall and septum of mouse embryo hearts are shown. (**E**) *Left panel:* No evidence of cellular hypertrophy or increased proliferation in *BANCR* positive embryo hearts as calculated by the percent of total cardiac ventricular area that stains positive for hematoxylin (nuclear stain). Note that % hematoxylin staining would *decrease* if cells exhibited hypertrophy as cytoplasmic volumes were relatively increased. *BANCR*-positive (*n* = 25 sections across 6 hearts), scramble control positive (*n* = 12 sections across 4 hearts), and plasmid-negative littermate controls (*n* = 19 sections across 6 hearts). One-way ANOVA, *P* value < 0.05. Error bars are +/- 1 s.e.m. All embryos were sectioned in the same orientation to avoid out-of-plane cellular distortion artifact. *Right panel:* No evidence of increased mitosis (Ki67+) among *BANCR* positive embryo hearts (*n* = 5 hearts), scramble control-positive (*n* = 2 hearts), or plasmid-negative littermate controls (*n* = 2 hearts). One-way ANOVA, *P* value < 0.05. Error bars are +/- 1 s.e.m. (**F**) GSEA of E16 embryo heart RNA-seq data. We observed enrichment of cellular respiration, cardiac muscle morphogenesis, and cardiac contraction pathways relative to littermate controls. False discovery rate (FDR) < 0.02. Top ten BOE-enriched pathways ranked by normalized enrichment score (NES) are shown. *n* = 2 biological replicates.

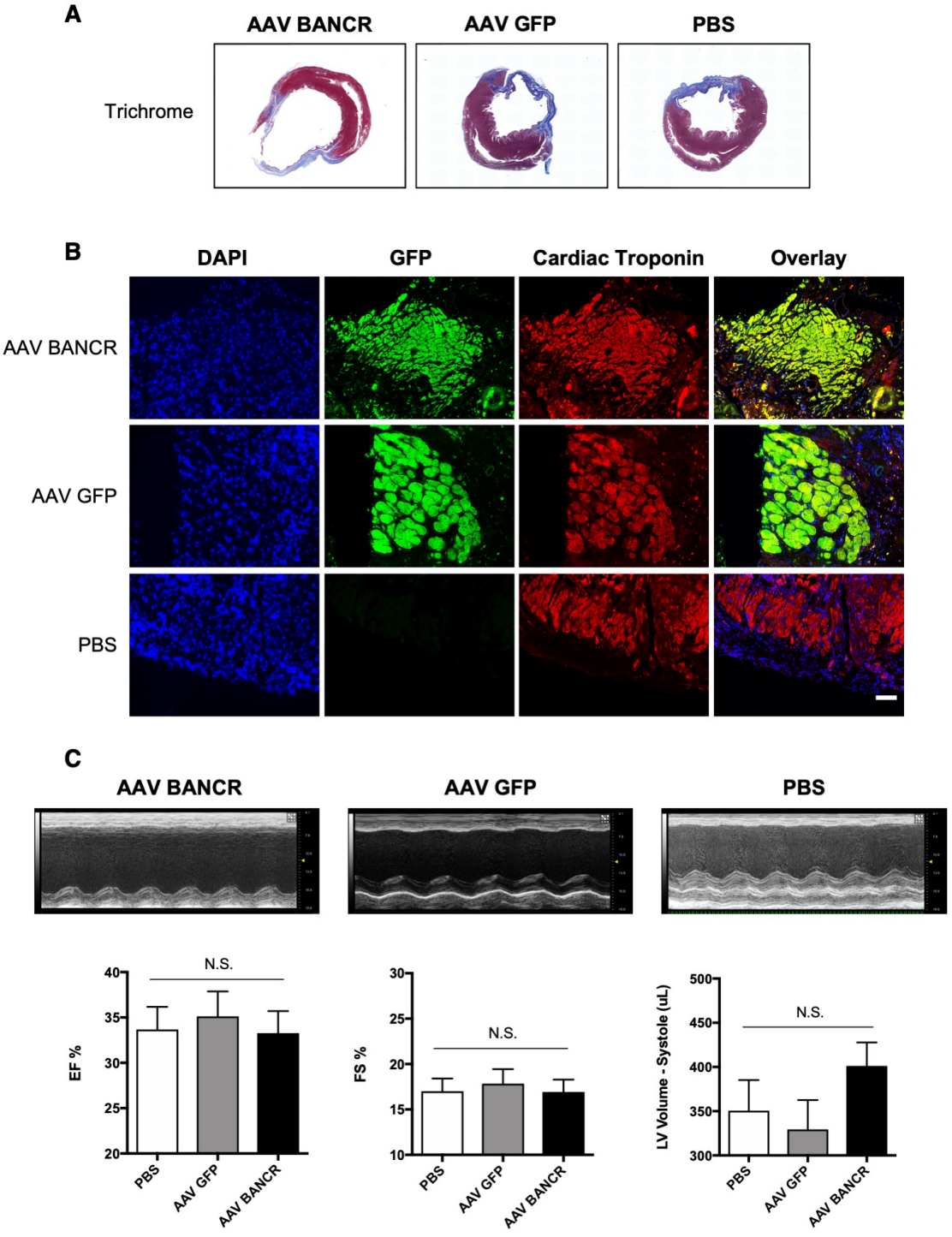

Supplementary Figure 7

Supplementary Figure 7. AAV9 injection of human *BANCR*-expressing plasmids into infarcted rat hearts. Related to Fig. 7I. (**A**) Representative Trichrome staining of explanted Sprague Dawley rat hearts at 5 weeks after left anterior descending (LAD) ligation and adeno-associated virus (AAV) direct injection. Significant dilation and infarction can be seen in the AAV BANCR group relative to the two control groups: AAV GFP and PBS. (**B**) GFP and cardiac Troponin immunostaining shows GFP+/Troponin+ cardiomyocytes in AAV BANCR and GFP hearts, but not PBS hearts. Scale bar = 40 μm. (**C**) Representative M-Mode left ventricular (LV) echocardiography images (top) and quantitative metrics (below) for AAV BANCR (n = 14 biological replicates) relative to AAV GFP (n = 9 biological replicates) and PBS (n = 9 biological replicates) controls. EF = ejection fraction; FS = fractional shortening. No significant changes are seen in these metrics, though systolic LV volume is trending towards significance. One-way ANOVA, P value < 0.05, error bars are +/- 1 s.e.m.

Supplementary Table 1

```
chr9:71911597-71921972_hg19         (human)
chr9:67848133-67858485_panTro4      (chimpanzee)
chr9:50813447-50824022_gorGor3      (gorilla)
chr9:63998480-64009095_ponAbe2      (orangutan)
chr15:78988508-78999116_rheMac      (rhesus macaque)
chr1:99809093-99815019_calJac3      (marmoset)
JH378181:4921103-4921282_saiBol1    (squirrel monkey)
Scaffold_1281:181891-187768_micMur1 (mouse lemur)
```

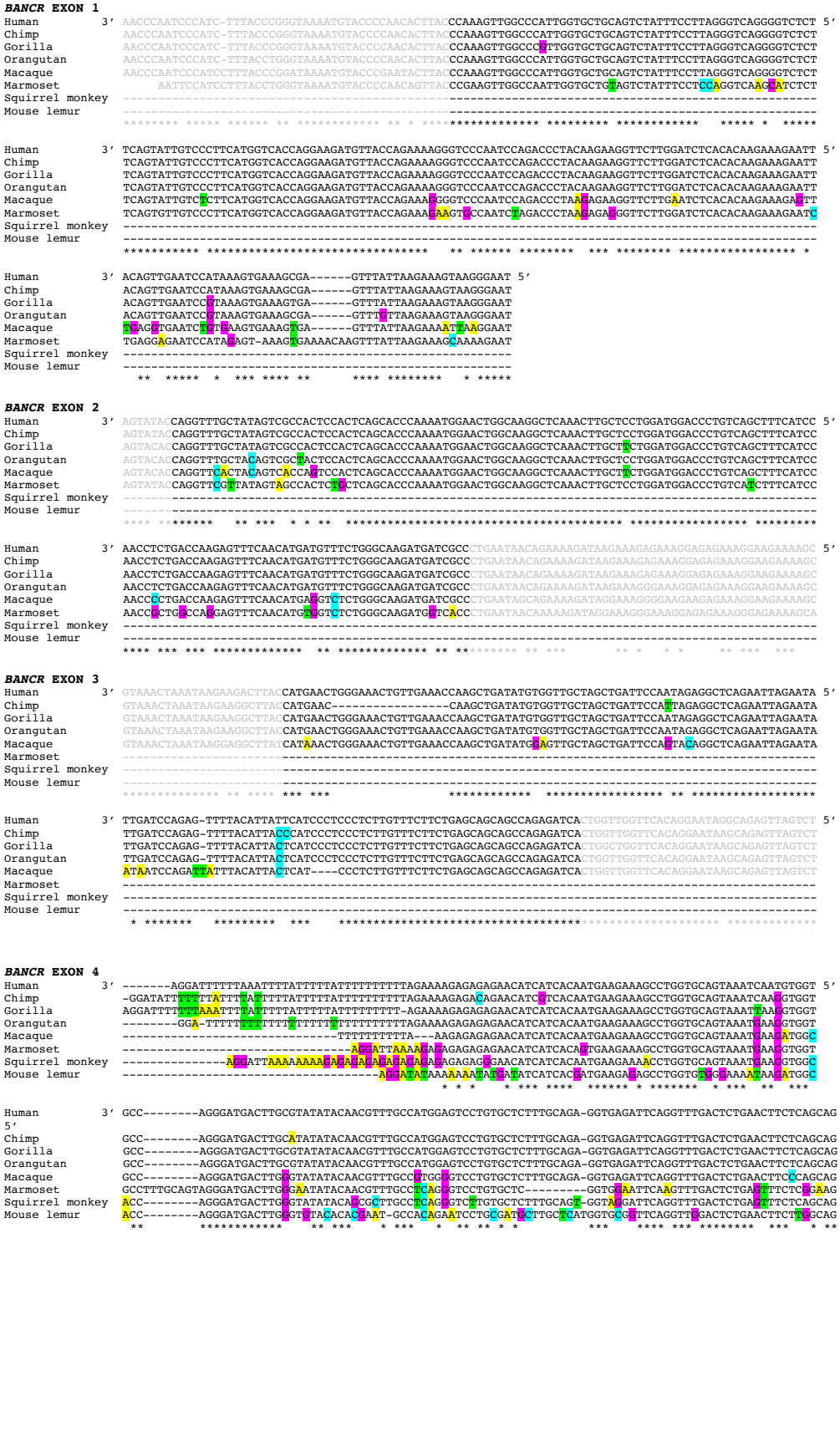

Supplementary Table 1. Sequence analysis of human *BANCR* exonic homologous regions in chimpanzee, gorilla, orangutan, rhesus macaque, marmoset, squirrel monkey, and mouse lemur. Related to Fig. 1D and 1E. Asterisks (*) indicate regions of 100% conservation among primates that have homologous exon sequence in that region. Colors denote non-human primate nucleotide base change from human reference: purple (guanine), green (thymine), yellow (adenine), and blue (cytosine).

Supplementary Table 2: JASPAR-predicted TBX5 binding sites wihtin 2 kb region upstream of BANCR							
Model ID	Model name	Score	Relative score	Start	End	Strand	predicted site sequence
MA0807.1	TBX5	9.322	0.914103078266245	731	738	-1	AGGTGTTG
MA0807.1	TBX5	9.322	0.914103078266245	1831	1838	-1	AGGTGTTG
MA0807.1	TBX5	9.297	0.913457057967217	1795	1802	-1	AGGGGTGA
MA0807.1	TBX5	9.001	0.905808177626719	1473	1480	-1	ATGTGTGA
MA0807.1	TBX5	8.031	0.88074259002441	76	83	1	ATGTGTTA
MA0807.1	TBX5	7.312	0.862163046224349	1752	1759	-1	AGGTGTTC
MA0807.1	TBX5	6.947	0.852731149858532	641	648	1	GGGTGTTT
MA0807.1	TBX5	6.942	0.852601945798726	119	126	1	AGGGGTGG
MA0807.1	TBX5	6.934	0.852395219303037	637	644	1	AGGTGGGT
MA0807.1	TBX5	6.505	0.841309510971707	218	225	1	TGGTGGGA
MA0807.1	TBX5	6.271	0.8352627609728	307	314	1	TGGTGTTG
MA0807.1	TBX5	5.862	0.824693868880692	1205	1212	-1	AAGTGCTA
MA0807.1	TBX5	5.689	0.820223408411415	340	347	1	TGGTGCTA
MA0807.1	TBX5	5.689	0.820223408411415	1759	1766	-1	TGGTGCTA
MA0807.1	TBX5	5.673	0.819809955420036	1022	1029	1	AGGTGATT
MA0807.1	TBX5	5.428	0.813478956489556	1525	1532	-1	AGATGTGA
MA0807.1	TBX5	5.410	0.813013821874256	1197	1204	-1	ATGTGTTT
MA0807.1	TBX5	5.403	0.812832936190528	1290	1297	-1	AGGTGGCT
MA0807.1	TBX5	5.300	0.81017133255853	193	200	-1	AAGTGCCA
MA0807.1	TBX5	5.191	0.807354684054766	1328	1335	1	AGGTGGGC
MA0807.1	TBX5	5.093	0.804822284482574	1501	1508	-1	GGGTGGGG

Supplementary Table 2. JASPAR TBX5 motif binding at 2 kb region upstream of *BANCR*. Related to Fig. 6. JASPAR-predicted TBX5 binding sites. A motif with high JASPAR score (9.322) located within the enhancer upstream of *BANCR* is highlighted in red.

Supplementary Table 3. Oligonucleotide sequences. Related to Key Resources.

Primer name	Sequence	Note
BANCRexon123_5'F_CRISPR	ATAACCATAAGTATCAACAG	BANCR exon 123 KO 5' CRISPR
BANCRexon123_5'R_CRISPR	CTGTTGATACTTATGGTTAT	BANCR exon 123 KO 5' CRISPR
BANCRexon123_3'F_CRISPR	AAGAAGACTTACCATGAACT	BANCR exon 123 KO 3' CRISPR
BANCRexon123_3'R_CRISPR	AGTTCATGGTAAGTCTTCTT	BANCR exon 123 KO 3' CRISPR
BANCRexon4_5'F_CRISPR	AGAAATGTGCACAGTAAAAC	BANCR exon 4 KO 5' CRISPR
BANCRexon4_5'R_CRISPR	GTTTTACTGTGCACATTTCT	BANCR exon 4 KO 5' CRISPR
BANCRexon4_3'F_CRISPR	GCTGAAACCAAAGTAGACAA	BANCR exon 4 KO 3' CRISPR
BANCRexon4_3'R_CRISPR	TTGTCTACTTTGGTTTCAGC	BANCR exon 4 KO 3' CRISPR
BANCR_EcoRI_exon4_F	GGGGGAATTCCTGCTGAGAAGTTCAGAGTCAA	exon4 overexpression plasmids F primer
BANCR_NotI_R	GGGGGCGGCCGCGGATCCGATTTAAATT	exon4 overexpression plasmids R primer
CRISPR_31F	AAGAAGCCAGCCTAAACCC	Verify CRISPR 31 clones
CRISPR_31R	TCATCTTTATGCCCATGAGTACC	Verify CRISPR 31 clones
CRISPR_4F	CTTTGAGCAATGTCTGGTTGTC	Verify CRISPR 4 clones
CRISPR_4R	GCTCTTGTAGAACTCAGCAGAA	Verify CRISPR 4 clones
BANCR_qPCR_F	TTCCTTAGGGTCAGGGGTCT	BANCR qPCR primers

BANCR_qPCR_R	GATTGGGACCCTTTTCTGGT	BANCR qPCR primers
BANCR_Enhancer_guide_RNA_1	AGAAGGTCGGCACAAGATAT	BANCR enhancer KO 5' CRISPR
BANCR_Enhancer_guide_RNA_2	TTAGCTCTGGAATTTTCCCC	BANCR enhancer KO 5' CRISPR
BANCR promoter Forward primer 5’	TTAGCGTATAATGAGCAGTGAGG	ChIP qRT-PCR
BANCR promoter Reverse primer 3’	GAGATAGAAGGTCGGCACAAG	ChIP qRT-PCR
BANCR enhancer Forward primer 5’	CTGCCTCAAGTACTCTCCTTAC	ChIP qRT-PCR
BANCR enhancer Forward primer 3’	CCAAGAGCTGGAATGCAAAG	ChIP qRT-PCR
ANKRD1-5’	GAGGGGAGGACAAGCTAACC	ChIP qRT-PCR
ANKRD1-3’	CGATGTGATCACCACCAAAG	ChIP qRT-PCR
CTGF-5’	GCCAATGAGCTGAA TGGAGT	ChIP qRT-PCR
CTGF-3’	CAATCCGGTGTGAGTTGATG	ChIP qRT-PCR